

Dynamical aspects of spontaneous symmetry breaking in driven flow with exclusion

S. L. A. de Queiroz

Instituto de Física, Universidade Federal do Rio de Janeiro, Caixa Postal 68528, 21941-972 Rio de Janeiro, Brazil

R. B. Stinchcombe

Rudolf Peierls Centre for Theoretical Physics, Clarendon Laboratory, University of Oxford, Oxford OX1 3PU, United Kingdom



(Received 26 February 2019; revised manuscript received 17 June 2019; published 26 July 2019)

We present a numerical study of a two-lane version of the stochastic nonequilibrium model known as the totally asymmetric simple exclusion process. For such a system with open boundaries, and suitably chosen values of externally imposed particle injection (α) and ejection (β) rates, spontaneous symmetry breaking can occur. We investigate the statistics and internal structure of the stochastically induced transitions or “flips,” which occur between opposite broken-symmetry states as the system evolves in time. From the distribution of time intervals separating successive flips, we show that the evolution of the associated characteristic times against externally imposed rates yields information regarding the proximity to a critical point in parameter space. On short timescales, we probe for the possible existence of precursor events to a flip between opposite broken-symmetry states. We study an adaptation of domain-wall theory to mimic the density reversal process associated with a flip.

DOI: [10.1103/PhysRevE.100.012141](https://doi.org/10.1103/PhysRevE.100.012141)

I. INTRODUCTION

Spontaneous symmetry breaking (SSB) is present in many systems studied both experimentally and theoretically. Some of the most relevant examples are magnetization reversal [1] and its close relative, domain nucleation [2] in two-dimensional Ising magnets, and (for fluids) flow reorientation and reversal in Rayleigh-Bénard convection [3–5].

For one-dimensional systems with finite-range interactions in thermal equilibrium at nonzero temperature T , it is well known that SSB is usually prevented by fluctuations. This may easily be seen for cases with discrete symmetry, such as the Ising model. Here the “modes” (differences of configurations possible at $T > 0$ from those at $T = 0$) are simple (domain walls) with system-size-dependent energy gap [6]. In the more subtle cases with continuous symmetry, the lower critical dimension for $T \neq 0$ phase transitions is raised by the soft character of the modes, according to the Goldstone argument [7]. These arguments do not apply to nonequilibrium systems. In particular, it has been predicted by mean-field theory, and verified by numerical simulations [8–12], that stochastic models in the family of the one-dimensional totally asymmetric simple exclusion process (TASEP) [13–19] do exhibit SSB in especially designed implementations.

The one-dimensional TASEP exhibits many nontrivial properties because of its collective character. It has been used, often with adaptations, to model a broad range of nonequilibrium physical phenomena, from the macroscopic level such as highway traffic [20] to the microscopic, including sequence alignment in computational biology [21] and current shot noise in quantum-dot chains [22].

In the time evolution of the $d = 1$ TASEP, the particle number n_ℓ at lattice site ℓ can be 0 or 1, and the forward hopping of particles is only to an empty adjacent site. In addition

to the stochastic character provided by random selection of site occupation update [23], the instantaneous current $J_{\ell\ell+1}$ across the bond from ℓ to $\ell + 1$ also depends on the stochastic attempt rate, or bond (transmissivity) rate, p_ℓ , associated with it. Thus,

$$J_{\ell\ell+1} = \begin{cases} n_\ell(1 - n_{\ell+1}) & \text{with probability } p_\ell \\ 0 & \text{with probability } 1 - p_\ell. \end{cases} \quad (1)$$

We take systems with open boundary conditions at both ends. In the usual formulation, each end is associated with an externally imposed, injection or ejection, attempt rate, respectively, α and β [13,16]. Considering a two-lane model [24,25], one allows two types of particles (denoted here by $+$ and $-$) such that, say, the $+$ particles move only from left to right, and the $-$ ones from right to left. Then one has two sets of external rates: $\{\alpha^+, \beta^+\}$ and $\{\alpha^-, \beta^-\}$. In order to enable SSB to arise, one must symmetrize the setup by making $\alpha^+ = \alpha^-$, $\beta^+ = \beta^-$. Details of the dynamics are given in Sec. II below. For the moment, we recall that the onset of SSB in the present case is inherently associated with the stochastic current and density fluctuations intrinsic to TASEP-like phenomena.

Our main goal here is to discuss dynamical aspects of the connection between fluctuations and SSB. For earlier work, see, especially, Refs. [26–28].

In Sec. II, we present the additional rules to be used here for two-lane TASEP, which make possible the onset of SSB. In Sec. III, we initially give details of the procedures used in our numerical simulations; then we analyze the time evolution of the TASEP model on long timescales, showing that for the values of (α, β) considered, the system exhibits an apparent steady state with broken symmetry. Stochastic fluctuations can induce a reversal, or “flip,” in the composition of the high- and low-density phases, between $+$ and $-$. On this timescale,

the flip is essentially instantaneous. We study the statistics of flips and its dependence on the external parameters by various methods. Next we turn to shorter timescales and investigate the internal structure of the aforementioned flips, both by direct visualization of simulational data and by probing for the possible existence of smaller “precursor” events to a full reversion in the composition of the high- and low-density phases. We present an adaptation of domain-wall theory to mimic the density reversal process associated with a flip. In Sec. IV, we summarize and discuss our results.

II. TASEP MODEL: THEORY

In line with Refs. [8,9], additionally to Eq. (1) for single-lane processes, we adopt the following rules for the coexistence (or not) between + and – particles:

(I) A + particle on the left and a – particle on the right of a bond can exchange places with probability $q > 0$: $+ - \Rightarrow - +$.

(II) At the left end, an injection attempt of a + particle can only take place if the first lattice site is empty of both + and – particles. Likewise for injection attempts of – particles into the last site at the right end.

It has been shown [8,9] that these conditions are sufficient to trigger SSB provided that the ejection attempt rate β is (i) less than α and (ii) suitably low; numerically, one needs $\beta \lesssim 1/3$ [8].

III. TASEP MODEL: NUMERICS

A. Introduction

We consider chains with N sites, $N - 1$ internal bonds, plus two so-called injection or ejection bonds at either extreme: to the left of the first site, where injection of + particles is attempted with rate α and ejection of – particles with rate β ; likewise to the right of site N , for ejection of + particles (β) and injection of – particles (α).

For a structure with $N_b = N + 1$ bonds, an elementary time step t_0 consists of N_b sequential bond update attempts, each of these according to the following rules: (1) select a bond at random, say, bond ij , connecting sites i and j ; (2) if the chosen bond has a site occupied by a + (–) particle on its left (right) and (2a) an empty site or (2b) a site occupied by a – (+) particle on its right (left), then (3) move the + (–) particle across it with probability (bond rate) p_{ij} in case (2a), or exchange + and – particles across the bond with probability q , in case (2b). If an injection or ejection bond is chosen, step (2) is suitably modified to account for the particle reservoir (the corresponding bond rate being, respectively, α or β); each time such bond is selected, the current state of occupation of the internal site to which it is attached determines whether it will be used for injection or ejection; see rule (II) of Sec. II.

Thus, in the course of one time step, some bonds may be selected more than once for examination and some may not be examined at all. This constitutes the *random-sequential update* procedure described in Ref. [23], which is the realization of the usual master equation in continuous time.

The sublattice parallel update process used in Ref. [28] is such that during one elementary step, all bonds are probed once and just once. The injection and ejection bonds are

treated exactly in the same way as here. It differs from our random-sequential process in that, as regards internal bonds, all (say) odd-numbered ones are updated with probability one and simultaneously (hence the “parallel” label attached); then, the even-numbered bonds undergo the same simultaneous update process. A moment’s reflection shows that exactly the same types of elementary moves, and site occupation states, are allowed both in our method and in theirs. The same can be said regarding the forbidden processes and site occupation states. So, on average over many steps, both processes give statistically equivalent results.

Here we use all internal bond rates $p_\ell = 1$ [see Eq. (1)] as well as $q = 1$; see rule (I) of Sec. II.

B. Flip statistics

We have focused on the region of the (α, β) parameter space where coexistence between high- and low-density phases (HD-LD) takes place, as that is where SSB effects are more intensely exhibited. For ease of comparison with extant results from Ref. [8], we start by taking $\alpha = 1, \beta = 0.15$, deep inside the HD-LD phase.

In addition to system-wide currents of \pm particles $J_\pm(t)$, we kept track of the position-averaged densities,

$$\rho_\pm(t) \equiv \frac{1}{N} \sum_{i=1}^N n_i^\pm(t), \quad (2)$$

where the $n_i^\pm(t)$ are a straightforward extension of the n_ℓ of Eq. (1) to systems with two particle species.

We generally started simulations with an empty lattice. After some time δt_{ss} , an apparent steady state exhibiting SSB is typically attained, in which the current and density differences, respectively, $\Delta J(t) \equiv J_+(t) - J_-(t)$ and $\Delta \rho(t) \equiv \rho_+(t) - \rho_-(t)$, are nonzero. Then, after some much longer interval $\delta t_{flip} \gg \delta t_{ss}$, a flip occurs in which ΔJ and $\Delta \rho$ concurrently reverse sign. As the system evolves stochastically, the high- and low-density coexisting phases alternate in composition between + and – particles, via successive flips.

In fact, even deep within the HD-LD coexistence region, a flip takes place over a succession of many elementary time intervals t_0 , as defined in the second paragraph of Sec. III A. So, one usually defines a “renormalized time” $t_r = N_r t_0$ and considers the quantities $J_\pm(t_r), \rho_\pm(t_r)$, which are averages of the instantaneous $J_\pm(t), \rho_\pm(t)$ over N_r consecutive elementary intervals t_0 .

Of course, in the thermodynamic limit $N \rightarrow \infty$, one expects the time taken for the system to switch between different symmetry-broken phases to diverge. Conclusive numerical evidence shows that the typical time between consecutive flips diverges exponentially in N for TASEP-like models such as the one studied here [8,28]. Thus, in what follows, we will generally concentrate on fixed, finite N and investigate the features exhibited in finite-size flip dynamics.

For $(\alpha, \beta) = (1, 0.15)$ with system size $N = 80$, using $N_r = 10^3$ gives a sharp definition of the “instant” (single value of t_r) when flips occur; see upper panel of Fig. 1. For higher $\beta = 0.20$ (but still well away from the transition from HD-LD to the symmetric phase) as shown in the lower panel of the figure, comparison with $\beta = 0.15$ shows the following: (i) a

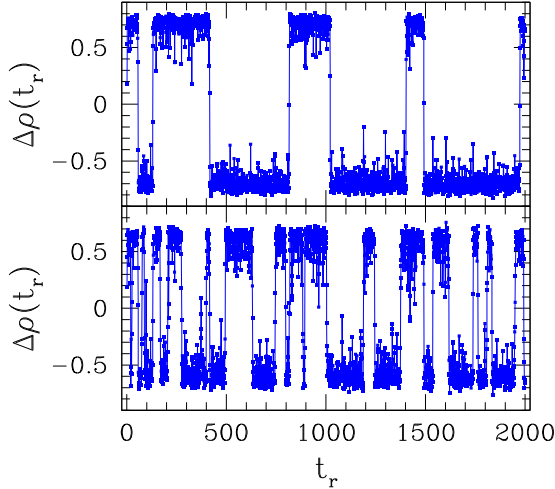


FIG. 1. Density differences $\Delta\rho(t_r)$ against renormalized time $t_r = 10^3 t_0$ for chain with $N = 80$ sites, $\alpha = 1$. Upper panel: $\beta = 0.15$; lower panel: $\beta = 0.20$. See text for definitions of t_r, t_0 .

reduction of the typical time Δt_r between consecutive flips; (ii) the appearance of “quasiflips,” in which $\Delta\rho$ goes slightly beyond zero but backtracks before full reversal; and (iii) the amplitude of flips slightly decreases, as generally expected for the order parameter of a system approaching a second-order phase transition (in this case, located at $\beta \approx 1/3$ [8]).

We performed a systematic investigation of point (i) by numerically evaluating the probability distribution functions (PDF) of the renormalized time intervals Δt_r for $\alpha = 1$ and $\beta = 0.15, 0.16, 0.175, 0.19$, and 0.20 . The results are shown in Fig. 2.

For all cases investigated, the distributions are very well fitted by a Poissonian form,

$$P(\Delta t_r) = \frac{1}{\tau_0} \exp\left(-\frac{\Delta t_r}{\tau_0}\right). \quad (3)$$

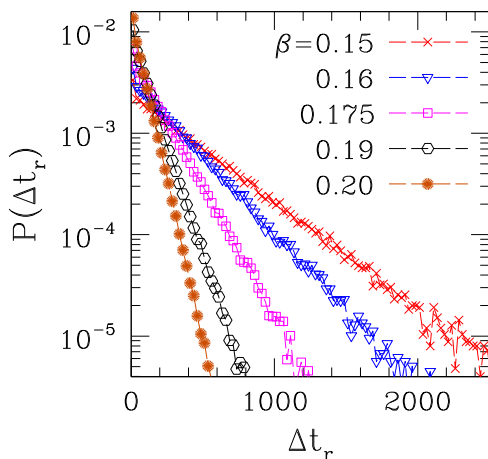


FIG. 2. For $\alpha = 1$ and assorted β in the HD-LD SSB phase, log-linear plots of numerically evaluated PDFs of renormalized time intervals Δt_r between consecutive flips for chain with $N = 80$ sites, $t_r = 10^3 t_0$. System size $N = 80$. See text for definitions of t_r, t_0 .

TABLE I. Results of fits of data shown in Fig. 2 to the Poissonian form, given by Eq. (3). See text for remarks on fit ranges and definition of numbers of events.

β	τ_0	Fit range	No. events
0.15	419 (2)	20–2500	50106
0.16	301 (2)	20–1900	71398
0.175	175 (1)	20–1500	123116
0.19	105 (2)	20–900	211726
0.20	72 (2)	20–750	308370

Poisson-like distributions for the time between consecutive flips have been found in Ref. [28], for a slightly different model whose main qualitative features are similar to those of the one studied here.

The β -dependent numerical values of the characteristic times τ_0 are given in Table I. Note that all fits exclude very short times, $\Delta t_r < 20$. This is because the so-called quasiflips defined above, while corresponding to very short-lived sign changes of $\Delta\rho$ without reaching full (quasistable) population reversion, tend to contaminate the statistics there (though they represent a very small fraction of the total number of sign-change events, for the interval of β under discussion; see the similar case of “spurious” magnetization reversals of two-dimensional Ising spin systems, treated in Ref. [1]).

Our samples were of total length 2×10^7 in units of t_r , so the last column in the table shows that the frequency of sign-change events remains rather low, reaching, at most, 1.5% for $\beta = 0.20$.

The decay of characteristic times τ_0 upon increasing β is fitted very closely by an exponential form, $\tau_0 \propto \exp(-\beta/\delta\beta_0)$, with $\delta\beta_0 \approx 0.029$. See Fig. 3(a), where the fitted curve is extended to higher β . At $\beta = 0.20 + 4\delta\beta_0 \approx 0.32$, the predicted value for τ_0 becomes of the order of one. Although that still corresponds to some 10^3 elementary updates, it is very small within the coarse-grained approach used

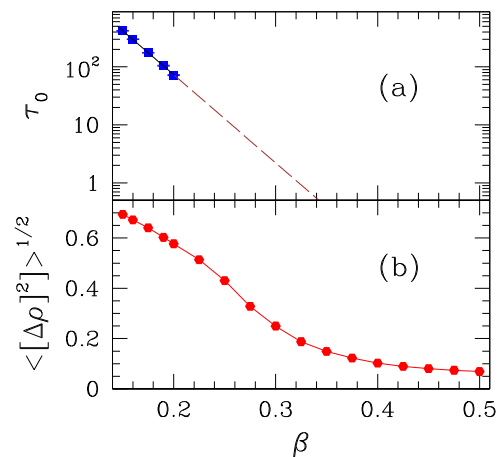


FIG. 3. (a) On a log-linear plot, the points are τ_0 from Table I; the line is the result of fitting data from the table to $\tau_0 \propto \exp(-\beta/\delta\beta_0)$, and is extended to $\beta > 0.20$ (dashed section). (b) Points are RMS values $\langle [\Delta\rho]^2 \rangle^{1/2}$ from simulations along (renormalized) time windows of width $t_r = 2000$, against β .

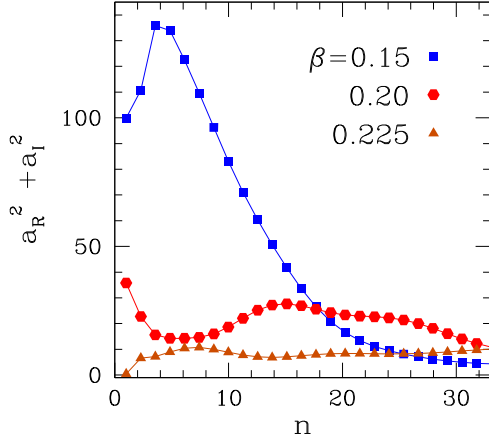


FIG. 4. For a chain with $N = 80$ sites, $\alpha = 1$ and varying β , low-frequency results from Fourier analysis of $\Delta\rho(t)$. a_R , a_I are, respectively, real and imaginary (frequency-dependent) components of Fourier transform. Frequencies are denoted by the label n ($f_n = nf_0/M$, with $n = 1, 2, \dots, M$; $f_0 = 1$ in units of inverse renormalized time, $M = 2048$).

in the analysis which produced the fitted data. Accordingly, it indicates that such picture of well-defined flips, separated by relatively long-lasting, quasistationary states of phase coexistence, is already breaking down by $\beta \approx 0.30$ or thereabouts. This is in broad agreement with $\beta_c \approx 1/3$ of Ref. [8].

In order to reach a better understanding of this behavior, we evaluated the averaged root-mean-square (RMS) values $([\Delta\rho]^2)^{1/2}$, where the angular brackets denote averages over a typical window of width $t_r = 2000$ (see, e.g., Fig. 1), for $\alpha = 1$, $0.15 \leq \beta \leq 0.50$. The results are shown in Fig. 3(b). It is seen that as β increases and the transition from HD-LD coexistence to a symmetric phase takes place, the contribution to $([\Delta\rho]^2)^{1/2}$ from the diminishing gap between majority and minority phases becomes smaller, and only the nonvanishing, intrinsic stochastic fluctuations remain. The change of behavior is signalled by the inflection of the curve, located in the vicinity of $\beta = 0.30$, again consistent with the preceding analysis and with Ref. [8].

We also applied Fourier analysis to our simulation data in order to quantify the properties of apparent periodic structures for the signal $\Delta\rho$, which can be seen, e.g., in the upper panel of Fig. 1. For $\alpha = 1$ and $0.15 \leq \beta \leq 0.225$, we concentrated on low frequencies and, for each β , closely examined the 32 largest-wavelength components over a total for $M = 2048$ sampled points. Our results are more easily conveyed with the help of the following procedures: (i) With $a_R(f)$, $a_I(f)$ being, respectively, the real and imaginary part of the Fourier transform at frequency f , we considered the powerlike quantity $a_R^2(f_n) + a_I^2(f_n)$ to represent the contribution of each frequency $f_n = nf_0/M$ to the observed signal (here, f_0 is the highest sampled frequency, equal to one unit of inverse renormalized time; $n = 1, 2, \dots, M$); (ii) with the help of standard graphics software, we smoothed out the resulting sequences of points in order to average out rapid oscillations and keep only the basic overall trends.

The results are displayed in Fig. 4 for $\beta = 0.15, 0.20$, and 0.225 . Comparison with the upper panel of Fig. 1 shows that

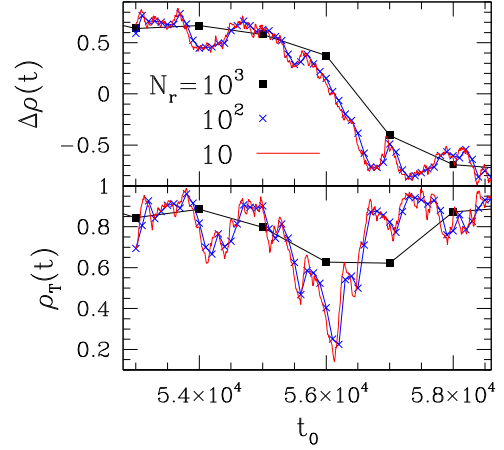


FIG. 5. Density differences $\Delta\rho(t)$ (upper panel) and total densities $\rho_T(t)$ (lower panel) against time t_0 in the vicinity of a flip for chain with $N = 80$ sites, $(\alpha, \beta) = (1, 0.15)$, as seen from averages taken over intervals of lengths $N_r t_0$, $N_r = 10^3, 10^2$, and 10 . See text for definition of t_0 .

for $\beta = 0.15$, the $n = 3$ and 4 modes (translating to oscillation periods of the order of 400 – 600 in renormalized time units) indeed have a strong contribution. For $\beta = 0.20$, there is a small but discernible maximum centered at frequencies around $n = 15$, which is roughly in line with the data from the lower panel of Fig. 1. For $\beta = 0.225$, no clear trend is visible.

The Poissonian character exhibited by the distributions of time intervals between flips strongly suggests that these are uncorrelated events, at least on long timescales. We now proceed to probing the complementary, short timescale in order to obtain detailed information on the structure and properties of the fluctuations involved in the overall switching between majority-population phases.

C. Flip structure

We begin by examining the features exhibited by a flip when it is seen on different timescales, i.e., for different values of $t_r = N_r t_0$ as defined above. We take $N = 80$, $(\alpha, \beta) = (1, 0.15)$. We refer to the leftmost $+ \rightarrow -$ flip in the top panel of Fig. 1, which takes place at $t_r \approx 50$ – 60 . In Fig. 5, we reproduce both $\Delta\rho(t)$ and the total density $\rho_T(t) = \rho_+(t) + \rho_-(t)$ in that time region, for $N_r = 10, 10^2$, and 10^3 . While the overall trend of $\Delta\rho(t)$ is already well represented by the $N_r = 10^3$ curve, the corresponding data for $\rho_T(t)$ miss out on a significant dip taking place around $t_0 = 5.6 \times 10^4$, which is captured by the $N_r = 10^2$ and 10 curves. Such an almost complete emptying of the lattice is indeed a qualitative feature broadly expected to take place during the flipping process [8,27,28].

Figure 6 shows $\Delta\rho(t)$ along a subsection of the time interval depicted in Fig. 5, now for $N_r = 10$ and unity. One sees that, in this case, no significant insight into the flipping process itself is gained by going to the shortest possible timescale. On such scale, for the values of α , β , and N used here, lattice discreteness effects show up to a large extent. Namely, plateaus are seen corresponding to time lapses

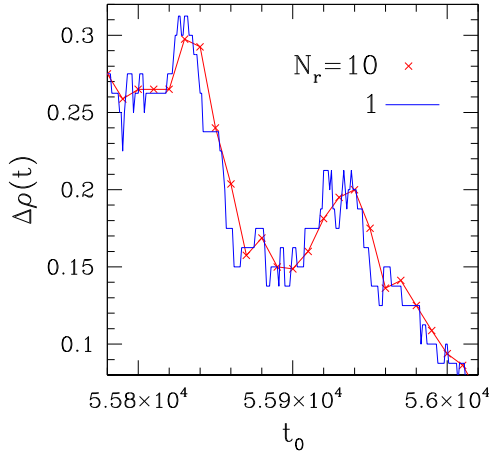


FIG. 6. Density differences $\Delta\rho(t)$ against time t_0 in the vicinity of a flip for chain with $N = 80$ sites, $(\alpha, \beta) = (1, 0.15)$, as seen from averages taken over intervals of length $N_r t_0$, $N_r = 10$ and 1. See text for definition of t_0 .

with no change in overall particle number [this is directly confirmed by analysis of the respective $\rho_T(t)$], as well as step-like variations in density-associated quantities. Discreteness effects would be reduced by going to larger N and/or higher β closer to $\beta_c \approx 1/3$ [8].

We investigated the possible existence of “precursor” events to flips. These, if at all present, would bear a qualitative similarity to the mechanism described in Refs. [27,28] in which, starting from an empty lattice, the system enters a symmetry-broken state through an “amplification loop” of initial fluctuations. In the present case, we specialize to flips from one symmetry-broken state to its opposite, for which inertial effects (absent for empty-lattice and other symmetric starting configurations) are expected to be paramount throughout the switching process.

Examination of the lower panel in Fig. 5 suggests that a reliable indicator for a flip is the steep descent of $\rho_T(t)$ towards a minimum value that is much lower than its long-time average away from flips, $\langle\rho_T\rangle$. We investigate the behavior of the two-time correlation (averaged over time t):

$$C(\tau) \equiv \left\langle \frac{d\rho_T(t+\tau)}{dt} (\rho_T(t) - \langle\rho_T\rangle) \right\rangle_t. \quad (4)$$

In order to capture the relevant fluctuations in the neighborhood of a flip, we consider both positive and negative τ , with $|\tau|$ not much larger than the average “duration” of a flip (i.e., the interval around the flip during which ρ_T differs significantly from its long-time average); this is estimated from Fig. 5 to be a couple-of-thousand times the elementary unit t_0 . For evaluation of the densities involved in Eq. (4), we used a renormalized timescale $t_r = 10^2 t_0$ and an interval of width $200 \leq \delta t \leq 800$ (in units of t_0) for numerical calculation of the time derivatives. The results from averaging over $N_{\text{sam}} = 10^4$ samples, i.e., consecutive values of t_r , are shown in Fig. 7. Because of the finite values of δt , all curves have peaks at $\tau = \pm\delta t/2$. Other than the central peaks just mentioned, one sees only a few small but well-defined secondary oscillations at larger $|\tau|$. The most relevant feature of the plots for our

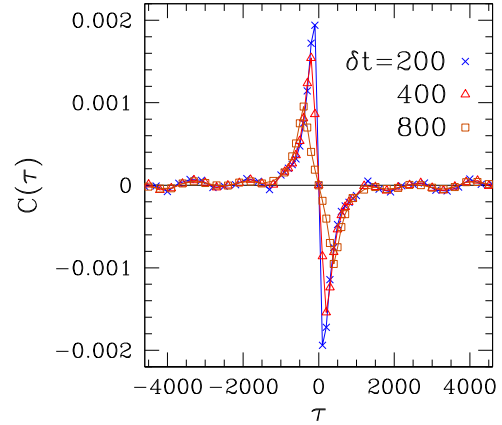


FIG. 7. Two-time correlation $C(\tau)$ of Eq. (4). Densities are averaged over $N_{\text{sam}} = 10^4$ time intervals of length $t_r = 10^2 t_0$. τ and δt are shown in units of t_0 . Chain with $N = 80$ sites, $(\alpha, \beta) = (1, 0.15)$. See text for definitions of N_{sam} , t_0 , δt .

current purposes is their remarkable degree of inversion symmetry around the origin, which strongly indicates that pre- and postflip fluctuations are, on average, equivalent. In other words, we have found no specific precursor events associated with a flip from one symmetry-broken state to its opposite.

It must be noted that the inversion symmetry exhibited in Fig. 7 reflects an ensemble average over many samples and is, in general, absent when one considers a single time interval, as shown in the bottom panel of Fig. 8. The distinctive shape of Fig. 7 only begins to emerge upon accumulation of at least a few tens of samples; see top panel of Fig. 8.

D. Domain-wall approach

We now investigate the extent to which an adaptation of domain-wall (DW) theory may be suitable for the present case. As is known [29–33], the DW approach incorporates fluctuations beyond the mean-field picture of TASEP. For one-dimensional systems with spatially uniform hopping and

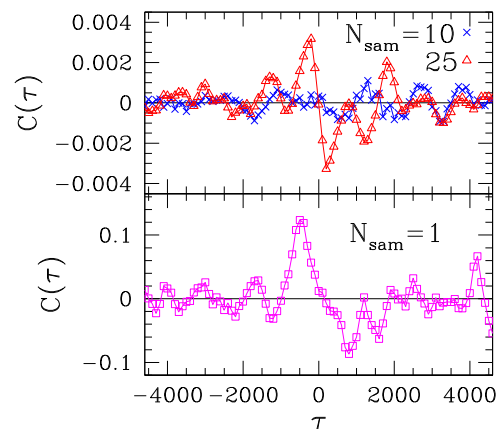


FIG. 8. Two-time correlation $C(\tau)$ of Eq. (4). Densities are averaged over time intervals of length $t_r = 10^2 t_0$, using $\delta t = 400$, with $N_{\text{sam}} = 10$ and 25 (top panel), or for a single sample, $N_{\text{sam}} = 1$ (bottom panel). τ and δt are shown in units of t_0 . Chain with $N = 80$ sites, $(\alpha, \beta) = (1, 0.15)$. See text for definitions of N_{sam} , t_0 , δt .

a single type of particle, it reproduces several exact results either exactly or to a very good numerical approximation. DW treatments have provided good quantitative account of nonstationary properties of single-species TASEP [32,33].

The flips between opposite symmetry-broken states exhibited by the systems studied here constitute an extreme case of cooperative behavior, though of course it originates in the usual (“microscopic”) stochastic mechanisms of the standard TASEP. On the other hand, the DW description corresponds to a “macroscopic” view of the system state. For the single-species case, this corresponds to a narrow domain wall separating a domain on the left side, with uniform site occupation (local density) ρ_L controlled by the injection rate, from another on the right with uniform site occupation ρ_R :

$$\rho_L = \alpha; \quad \rho_R = 1 - \beta. \quad (5)$$

The mean-field currents in the two domains are, respectively,

$$J_L = \alpha(1 - \alpha); \quad J_R = \beta(1 - \beta). \quad (6)$$

However, these steady-state currents do not balance at the domain wall, if it is stationary. This indicates the need to allow for stochastic motion of the domain wall. One postulates that the TASEP process can be represented by the stochastic hopping of the domain wall, with asymmetric hopping rates D_L, D_R given by

$$\begin{aligned} D_L &= \frac{J_L}{\Delta\rho} = \frac{\alpha(1 - \alpha)}{1 - \alpha - \beta}, \\ D_R &= \frac{J_R}{\Delta\rho} = \frac{\beta(1 - \beta)}{1 - \alpha - \beta}, \end{aligned} \quad (7)$$

where $\Delta\rho \equiv \rho_R - \rho_L = 1 - \alpha - \beta$.

So the fluctuations present in DW theory arise from current and density mismatches induced by boundary conditions [29–31].

In this context, one sees that the way to mimic a flip would be by starting the evolution of two domain walls, one for each species, driven by boundary conditions corresponding to a specific majority species, say + particles, and allowing the system to reach a steady state; then, suddenly switch the boundary conditions to those appropriate to the opposite majority species. The dynamics of the approach to a new steady state under a sudden change in boundary conditions has been investigated in Ref. [32] for the single-species TASEP.

The fact remains, however, that we will be switching from one fixed set of boundary conditions to a different, but also fixed, one. It is not clear from the outset how this affects the description of the flipping process, which is one that involves detailed local adjustment to constantly changing, stochastically determined microscopic fluctuations.

In line with DW theory, one starts with the mean-field densities and currents for each species, with adaptations for the coupling at the injection points. For completeness, we reproduce results from Ref. [8] in Eqs. (8)–(11) below. With

$$\begin{aligned} J^+ &= \alpha(1 - n_1^+ - n_1^-) = \beta n_N^+, \\ J^- &= \alpha(1 - n_N^+ - n_N^-) = \beta n_1^-, \end{aligned} \quad (8)$$

and defining

$$\begin{aligned} \alpha^+ &= \frac{\alpha(1 - n_1^+ - n_1^-)}{1 - n_1^+} = \frac{J^+}{J^+/\alpha + J^-/\beta}, \\ \alpha^- &= \frac{\alpha(1 - n_N^+ - n_N^-)}{1 - n_N^-} = \frac{J^-}{J^-/\alpha + J^+/\beta}, \\ \beta^+ &= \beta^- = \beta, \end{aligned} \quad (9)$$

one gets two single-species processes within the mean-field approximation. Specializing to the HD-LD phase and assuming the + particles to be in the majority, one finds

$$\alpha^- = \frac{1 + \alpha}{2} - \frac{1}{2}\sqrt{(1 + \alpha)^2 - 4\alpha\beta}. \quad (10)$$

For this case, the currents and respective densities in the bulk are

$$\begin{aligned} J^+ &= \beta(1 - \beta); \quad \rho^+ = 1 - \beta, \\ J^- &= \alpha^-(1 - \alpha^-); \quad \rho^- = \alpha^-. \end{aligned} \quad (11)$$

The corresponding expression for α^+ can be found from Eq. (9).

So for the two single-species processes with the + species in the majority, Eqs. (5) and (6) translate into

$$\begin{aligned} \rho_L^+ &= \alpha^+; \quad \rho_R^+ = 1 - \beta; \\ J_L^+ &= \alpha^+(1 - \alpha^+); \quad J_R^+ = \beta(1 - \beta), \end{aligned} \quad (12)$$

$$\begin{aligned} \rho_L^- &= \alpha^-; \quad \rho_L^- = 1 - \beta; \\ J_R^- &= \alpha^-(1 - \alpha^-); \quad J_L^- = \beta(1 - \beta). \end{aligned} \quad (13)$$

The hopping rates $D_{L,R}^\pm$ follow from plugging Eqs. (12) and (13) into Eqs. (7).

For the case with the – species in the majority, it is α^+ which is given by Eq. (10); Eq. (11) turns into

$$\begin{aligned} J^- &= \beta(1 - \beta); \quad \rho^- = 1 - \beta, \\ J^+ &= \alpha^+(1 - \alpha^+); \quad \rho^+ = \alpha^+. \end{aligned} \quad (14)$$

Similarly, the new α^- is found from Eq. (9) with the J^+, J^- from Eq. (14).

We started the DW evolution with the $D_{L,R}^\pm$ corresponding to the + species majority and waited some time t_{sst} until the system reached a steady state. This can be ascertained by checking whether the density profiles $\rho_\pm(n)$ (where $n = 1, \dots, N$ denotes the site position along the chain) remain stationary. The definition of “time” (t^{DW}) in this case comes up in that one solves the discrete-time version of the (continuous-time) differential equation for the DW position. Then the elementary time interval dt separates consecutive lattice-wide updates of the probability distribution $P(x, t)$ of finding the DW at the bond between sites $x = n$ and $x = n + 1$ at time t . See Ref. [33] for a discussion of this point. Here we used $dt = 1$, which corresponds to equivalence between t^{DW} and the elementary simulational time t_0 as defined in Sec. III A.

For $(\alpha, \beta) = (1, 0.15)$ and $N = 80$ sites, we saw that $t_{\text{sst}} \approx 10^4$ is enough to reach a steady state to very good accuracy. We then reset the clock and switched to boundary conditions such that the – species majority became favored. Figure 9 shows density profiles at specific times of interest.

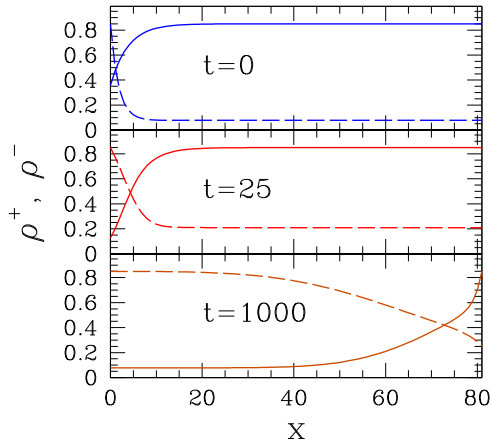


FIG. 9. Density profiles for + particles (full lines) and - particles (dashed lines) predicted by DW. At $t = 0$ (upper panel), these are the steady-state ones for a high density of + particles. Then boundary conditions are instantaneously switched. Note the rapid increase in bulk density of - particles for very short times (middle panel). By $t = 1000$ (lower panel), the profiles are on the way to their new steady-state configurations. $(\alpha, \beta) = (1, 0.15)$. Chain with $N = 80$ sites at $x_n = n$, $n = 1, \dots, N$ in lattice parameter units.

At $t = 0$ when boundary conditions are switched (top panel), the profiles are the steady-state ones predicted by DW for + particles in the majority. In the initial steps of evolution according to the new boundary conditions, there is a very rapid inflow of - particles: their bulk density away from the left boundary goes from $\rho^- = 0.07805$ (top panel) to $\rho^- = 0.20998$ (middle panel) by $t = 25$. This is not accompanied by an equally dramatic emptying of the + density, so initially the total density ρ_T actually grows. Most of the change takes place in a step-function shape during the very first full-lattice update, at the end of which the density variations have been $\delta\rho^+ = -0.0063$, $\delta\rho^- = 0.1310$. The lower panel of the figure is for $t = 1000$, which corresponds to the minimum value of ρ_T during the flipping process; see Fig. 10. By $t = 3000$ (not shown), the profiles have become very close to their new steady-state configuration, with deviations down to, at most, 0.05% (this latter value corresponds to the new majority - particles, near their injection end).

Figure 10 depicts the evolution of $\Delta\rho$ and ρ_T , showing that both of these quantities become very close to their values associated with the new steady state by $t^{\text{DW}} \approx 2500$; so this can be broadly defined as the “duration” of the flip, as given by the DW approach just described.

Recall that from the simulational results depicted in Fig. 5, one gets an estimate of $\approx 2 \times 10^3$ in units of t_0 for the duration of the flip exhibited there. Thus, accepting the identification of t^{DW} with t_0 as argued above (see also Ref. [33]), this means that both in our implementation of DW and in numerical simulations the flip duration is of the same order of magnitude, when measured in the respective “time” units.

On the other hand, it is seen in the lower panel of Fig. 10 that the minimum value attained by the total density along the flipping process is $\rho_T \approx 0.88$, only 6% below its steady-state counterpart. This is a large discrepancy against the simulational result shown in Fig. 5, where $\rho_T \approx 0.2$ at the bottom

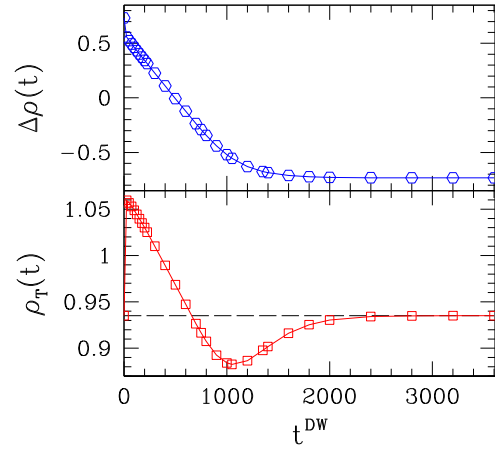


FIG. 10. Density differences $\Delta\rho(t)$ (upper panel) and total densities $\rho_T(t)$ (lower panel) against time t^{DW} after boundary conditions are switched (see Fig. 9 and text) for chain with $N = 80$ sites, $(\alpha, \beta) = (1, 0.15)$. The dashed line in the lower panel indicates $\rho_T(0)$.

of the dip is less than a quarter of the steady-state value. So the “emptying” of the lattice, which is widely accepted as having a paramount role in the flipping mechanism (see Refs. [8,27,28] as well as the results shown in Figs. 5 and 6 above), turns out to be a quantitatively minor feature in the DW result.

Of course, as stated above, here we are mimicking a flip; the present result indicates that the tools provided by DW theory do not fully emulate the large microscopic fluctuations driving a “real” flip. Incidentally, it should be noted that DW steady-state profiles, such as those on the top panel of Fig. 9, are in good agreement with both mean-field and simulational results [8].

IV. DISCUSSION AND CONCLUSIONS

In this paper, we studied the statistics and internal structure of the so-called flips exhibited by a specific implementation of a two-lane, two-species TASEP process in space dimensionality $d = 1$, which follows the rules given in Secs. I and II. We focused on the region of the (α, β) parameter space where coexistence between high-density and low-density (HD-LD) phases occurs. The above-mentioned flips consist of fluctuation-induced exchanges in composition of HD and LD phases (i.e., between opposite broken-symmetry states of the two-species system). This being a *bona fide* SSB phenomenon, the time between successive flips diverges in the thermodynamic limit. Thus we considered only chains with a finite number N of sites.

Initially, we looked at timescales much longer than the typical duration of a flip. We took the renormalized timescale $t_r = N_r t_0$, where t_0 is the elementary time step corresponding to a full (stochastic) sequential lattice update, with $N_r = 10^3$. On such scale, the flips are essentially “instantaneous” for the values of (α, β) and N used. We collected the statistics of the times Δt_r elapsed between consecutive flips. For fixed $N = 80$, $\alpha = 1$, β in $[0.15, 0.20]$, we found the distribution of the Δt_r to be Poissonian with β -dependent characteristic

times $\tau_0(\beta)$, indicating that flips are uncorrelated events on long timescales.

We showed in Fig. 3 how the evolution of the $\tau_0(\beta)$ is a good indicator of where in (α, β) parameter space a second-order transition is to be expected (in this case, the transition HD-LD \rightarrow LD [8]).

Fourier analysis of our time sequences of $\Delta\rho(t)$ (see Fig. 4) shows clear evidence of some apparent periodic, low-frequency structures in our simulation results for $\alpha = 1$, $\beta = 0.15$. For $\beta = 0.20$, one can still distinguish a small maximum in the weight for larger-frequency components, again consistent with visual inspection of the raw data. At $\beta = 0.225$ (closer to the transition at $\beta \approx 1/3$), our Fourier transform results show no clear trend.

In order to exploit the internal structure of flips, we then went to shorter timescales, using $N_r = 1, 10$, and 10^2 ; see Figs. 5 and 6. By doing so, one detects relevant features which may be lost in averages over scales for which flips are instantaneous. For $N_r \leq 10^2$, one clearly sees the emptying of the lattice, which is a qualitative feature broadly expected to be an integral part of the flipping process [8,27,28].

It is important to recall that the quantities exhibited in Figs. 5 and 6 are always position-averaged particle densities (or density differences). Dealing with lattice-averaged quantities proved invaluable in that it enabled us to work with smoothly varying functions of time.

We attempted to look at the details of what happened at individual sites or even short subsections of the system; however, the sample-to-sample fluctuations were so large as to prevent any clear conclusions to be drawn.

We evaluated and analyzed especially designed two-time correlations which might be expected to be sensitive to asymmetries between the time intervals before and after a flip takes place. Such precursor events, if detected, would be qualitatively similar to the mechanism described in Refs. [27,28]. In that case, it was shown that an initially empty lattice (or any other initially symmetric configuration) is led into a symmetry-broken state through an amplification loop of

initial fluctuations. An important difference is that in our case, we studied flips between broken-symmetry states. We found strong indications that pre- and postflip fluctuations are essentially equivalent (see Fig. 7); no sign was found of precursor events to flips.

On a complementary note to the discussion of lattice-averaged densities two paragraphs above, we were able to get reasonably smooth data even for a “single” sample of $C(\tau)$ (see the bottom panel of Fig. 8) because the quantity under observation depended only on the evolution of the position-averaged density (although it involved a short-time interval).

We also used a domain-wall (DW) approach to mimic a flip, by suddenly reversing the boundary conditions applied to a system in an SSB steady state. One notable feature emerging from the DW evolution is that the overall duration of the flipping process is similar, when measured in the respective time units (t^{DW}), to that of a simulationally generated flip (measured in computational time t_0).

On the other hand, the DW evolution fails to provide a quantitatively adequate account of the lattice emptying process which has been seen in simulations, and which is theoretically understood to be a fundamental component of the flipping process. Numerically, in the DW description, the total density goes through a minimum that is only a few percentage points below its steady-state value, while simulations would lead one to expect a typical maximum dip of the order of 70–80% (for the same α, β , and N). See Fig. 10.

ACKNOWLEDGMENTS

S.L.A.d.Q. thanks the Rudolf Peierls Centre for Theoretical Physics, Oxford, for hospitality during his visit. The research of S.L.A.d.Q. is supported by the Brazilian agencies Conselho Nacional de Desenvolvimento Científico e Tecnológico (Grant No. 303891/2013-0) and Fundação de Amparo à Pesquisa do Estado do Rio de Janeiro (Grants No. E-26/102.760/2012, No. E-26/110.734/2012, and No. E-26/102.348/2013).

-
- [1] K. Brendel, G. T. Barkema, and H. van Beijeren, *Phys. Rev. E* **67**, 026119 (2003).
 - [2] K. Brendel, G. T. Barkema, and H. van Beijeren, *Phys. Rev. E* **71**, 031601 (2005).
 - [3] K. R. Sreenivasan, A. Bershadskii, and J. J. Niemela, *Phys. Rev. E* **65**, 056302 (2002).
 - [4] R. Benzi, *Phys. Rev. Lett.* **95**, 024502 (2005).
 - [5] E. Brown and G. Ahlers, *J. Fluid Mech.* **568**, 351 (2006); H.-D. Xi, Y.-B. Zhang, J.-T. Hao, and K.-Q. Xia, *ibid.* **805**, 31 (2016).
 - [6] R. Peierls, *Proc. Camb. Philos. Soc.* **32**, 477 (1936).
 - [7] J. Goldstone, *Nuovo Cimento* **19**, 154 (1961); N. D. Mermin and H. Wagner, *Phys. Rev. Lett.* **17**, 1133 (1966).
 - [8] M. R. Evans, D. P. Foster, C. Godrèche, and D. Mukamel, *Phys. Rev. Lett.* **74**, 208 (1995); *J. Stat. Phys.* **80**, 69 (1995).
 - [9] V. Popkov, M. R. Evans, and D. Mukamel, *J. Phys. A* **41**, 432002 (2008).
 - [10] C. Appert-Roland, H. J. Hilhorst, and G. Schehr, *J. Stat. Mech.: Theory Expt.* (2010) P08024.
 - [11] N. Sharma and A. K. Gupta, *J. Stat. Mech.: Theory Expt.* (2017) 043211.
 - [12] A. K. Verma, N. Sharma, and A. K. Gupta, *Phys. Rev. E* **97**, 022105 (2018).
 - [13] B. Derrida, *Phys. Rep.* **301**, 65 (1998).
 - [14] G. M. Schütz, in *Phase Transitions and Critical Phenomena*, edited by C. Domb and J. L. Lebowitz (Academic, New York, 2000), Vol. 19.
 - [15] B. Derrida, E. Domany, and D. Mukamel, *J. Stat. Phys.* **69**, 667 (1992).
 - [16] B. Derrida, M. R. Evans, V. Hakim, and V. Pasquier, *J. Phys. A* **26**, 1493 (1993).
 - [17] R. B. Stinchcombe, *Adv. Phys.* **50**, 431 (2001).
 - [18] R. A. Blythe and M. R. Evans, *J. Phys. A* **40**, R333 (2007).
 - [19] T. Chou, K. Mallick, and R. K. P. Zia, *Rep. Prog. Phys.* **74**, 116601 (2011).
 - [20] B. Schmittmann and R. K. P. Zia, in *Phase Transitions and Critical Phenomena*, edited by C. Domb and J. L. Lebowitz (Academic, New York, 1995), Vol. 17.

- [21] R. Bundschuh, *Phys. Rev. E* **65**, 031911 (2002).
- [22] T. Karzig and F. von Oppen, *Phys. Rev. B* **81**, 045317 (2010).
- [23] N. Rajewsky, L. Santen, A. Schadschneider, and M. Schreckenberg, *J. Stat. Phys.* **92**, 151 (1998).
- [24] D. Chowdury, L. Santen, and A. Schadschneider, *Phys. Rep.* **329**, 199 (2000).
- [25] D. Helbing, *Rev. Mod. Phys.* **73**, 1067 (2001).
- [26] G. M. Schütz, *J. Phys. A* **36**, R339 (2003).
- [27] R. D. Willmann, G. M. Schütz, and S. Großkinsky, *Europhys. Lett.* **71**, 542 (2005).
- [28] S. Großkinsky, G. M. Schütz, and R. D. Willmann, *J. Stat. Phys.* **128**, 587 (2007).
- [29] A. B. Kolomeisky, G. M. Schütz, E. B. Kolomeisky, and J. P. Straley, *J. Phys. A* **31**, 6911 (1998).
- [30] V. Popkov and G. M. Schütz, *Europhys. Lett.* **48**, 257 (1999).
- [31] M. Dudzinsky and G. M. Schütz, *J. Phys. A* **33**, 8351 (2000).
- [32] L. Santen and C. Appert, *J. Stat. Phys.* **106**, 187 (2002).
- [33] R. B. Stinchcombe and S. L. A. de Queiroz, *Phys. Rev. E* **94**, 012105 (2016).